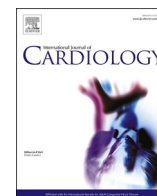| Title	Ratio of pulmonary artery diameter to ascending aortic diameter and its association with right ventricular failure after left ventricular assist device implantation
Author(s)	Chimura, Misato; Ohtani, Tomohito; Sera, Fusako et al.
Citation	International Journal of Cardiology. 2025, 418, p. 132596
Version Type	VoR
URL	https://hdl.handle.net/11094/98581
rights	This article is licensed under a Creative Commons Attribution 4.0 International License.
Note	

Contents lists available at ScienceDirect

International Journal of Cardiology

Ratio of pulmonary artery diameter to ascending aortic diameter and its association with right ventricular failure after left ventricular assist device implantation

Misato Chimura [a], Tomohito Ohtani [a,*], Fusako Sera [a], Kei Nakamoto [a], Yasuhiro Akazawa [a], Kenji Kajitani [a], Rie Higuchi [a], Toshifumi Kagiya [b], Yasushi Sakata [a]

[a] *Department of Cardiovascular Medicine, Osaka University Graduate School of Medicine, Suita, Japan*
[b] *Imperial Hotel Clinic Osaka, Osaka, Japan*

ARTICLE INFO

ABSTRACT

Background: Several invasive hemodynamic parameters help predict right ventricular failure (RVF) after left ventricular assist device (LVAD) implantation. However, prediction using non-invasive parameters alone has not been established. The ratio of the diameters of the pulmonary artery (PAD) to those of the ascending aorta (AoD) may indicate past hemodynamic load and cardiac dysfunction. We aimed to investigate a predictive model for RVF after LVAD implantation using non-invasive parameters including PAD/AoD ratio.
Methods: We studied 141 patients who underwent primary LVAD implantation and 117 healthy individuals with computed tomography (CT) data. RVF was defined as the need for a subsequent right ventricular assist device or intravenous inotrope administration for more than 30 days after LVAD implantation. The PAD/AoD ratio was measured at the level of the pulmonary artery bifurcation on the CT transaxial slices.
Results: RVF was observed in 29 patients. The correlation between PAD and AoD differed among healthy individuals, patients with and without RVF. Patients with RVF had higher total bilirubin and log brain natriuretic peptide (BNP) levels, a lower left ventricular end-diastolic diameter (LVDd) index, and a higher PAD/AoD ratio than those without RVF. Decision tree analysis indicated that the subgroup with a high PAD/AoD ratio ($\geq$1.09) and a small LVDd index ($<$35.4 mm/m^2) showed the highest probability of RVF (100 %), while the subgroup with a low PAD/AoD ratio ($<$1.09) and low log BNP ($<$2.79) showed the lowest probability of RVF (1 %).
Conclusion: Combining non-invasive parameters with the PAD/AoD ratio can predict RVF with high accuracy.

1. Introduction

Left ventricular assist devices (LVAD) have been used to treat patients with advanced heart failure (HF) for two decades [1–3]. The number of patients undergoing LVAD implantation has dramatically increased [4]. However, some patients undergoing LVAD implantation experience right ventricular failure (RVF), resulting in significant morbidity and mortality [5]. In particular, RVF is a critical issue in destination therapy, which aims to improve the quality of life by supporting left ventricular function using LVAD alone. Right ventricular (RV) dysfunction involves hemodynamically dependent factors, such as

increased preload and/or afterload to the RV, and hemodynamic-independent myocardial dysfunction, such as dysfunction caused by non-ischemic or ischemic cardiomyopathy, leading to RVF after LVAD [6–8]. Risk scores for predicting RVF, such as the EUROMACS-RHF score, which contains preoperative hemodynamic parameters, have been reported to be helpful clinically [9,10]. However, these scores are not always suitable for screening for RVF because hemodynamic parameters, such as the ratio of right atrial pressure (RAP) to pulmonary artery wedge pressure (PAWP), must be obtained invasively by right heart catheterization (RHC). A definitive indicator to assess hemodynamic-independent myocardial dysfunction of the RV after

---

LVAD therapy has not yet been well established.

We previously reported an association between aortic diameter (AoD) and pulmonary artery diameter (PAD), as assessed by non-contrast computed tomography (CT) images, and short-term prognosis in patients with dilated cardiomyopathy (DCM) and severe HF [11]. Patients with DCM and a long history of low stroke volume exhibited a remarkably small AoD, while those with a long history of postcapillary pulmonary hypertension (PH) showed a mildly enlarged PAD, resulting in a significantly higher PAD/AoD ratio than that of the controls. Moreover, these indices were not altered by temporary hemodynamic changes. Hemodynamically independent cardiac dysfunction is a component of RVF development, as is hemodynamically dependent cardiac dysfunction. Therefore, we hypothesized that the PAD/AoD ratio may reflect information on current hemodynamically independent cardiac dysfunction caused by long-standing hemodynamic loading and help identify patients at high risk for RVF after LVAD. This study aimed to evaluate the associations between non-invasive preoperative parameters, including the PAD/AoD ratio, and the incidence of RVF after LVAD implantation and to establish a non-invasive prediction model for RVF.

2. Methods

2.1. Study participants

We screened 188 patients who underwent primary LVAD implantation between April 2011 and February 2022 at Osaka University Hospital. Thirteen patients were excluded due to the lack of technically evaluable CT images, whereas 29 patients were excluded due to the absence of CT images within 90 days prior to LVAD implantation. Additionally, four patients were excluded because of the absence of echocardiographic examination data within 30 days prior to LVAD implantation, and one patient was excluded because of the lack of plasma brain natriuretic peptide (BNP) data within 16 days before LVAD implantation. Ultimately, 141 patients who underwent primary LVAD implantation were included in the analysis. Clinical and laboratory data, including plasma brain natriuretic peptide (BNP) and medication data, were collected as the most recent data (median of 1 day, 25th, and 75th percentiles 0 and 4 days) before LVAD implantation. RVF was defined as the need for a subsequent right ventricular assist device (RVAD) and intravenous inotropes for more than 30 days after LVAD implantation [12]. RVF was classified into two subtypes: early acute RVF and early post-LVAD RVF. Following a previous report [13], early acute RVF was defined as RVAD implantation concomitant with LVAD implantation in the operating room, whereas all the other cases of RVF were categorized as early post-LVAD RVF. The timing of the LVAD implantation was determined by the institutional heart team. Device types were also determined by the institutional heart team based on the patients' body shape and size at the time of LVAD implantation. A total of 53 patients (38 %) were implanted with HeartMate II, 2 (16 %) with HeartMate III, 9 (6 %) with DuraHeart, 23 (16 %) with HVAD, 14 (10 %) with Jarvik 2000, 15 (11 %) with EVAHEART, and 4 (3 %) with EVAHEART II.

To evaluate normal AoD and PAD values, we selected 117 healthy individuals who underwent medical examinations at the Imperial Hotel Clinic, Osaka, between January 2017 and September 2018. These individuals had no history of illness and showed no abnormal findings in blood pressure, laboratory tests, echocardiographic examinations, or CT images.

This study adhered to the tenets of the Declaration of Helsinki and Good Clinical Practice. The personal information concerning research was managed by assigning anonymized numbers unrelated to the personal information of the research subjects beforehand. This study was approved by the local ethics committee of Osaka University Hospital (No. 19210) and Omichikai Social Medical Corporation (No. T-2). All patients were provided the opportunity to refuse participation through a public opt-out mechanism. This study is in compliance with the ISHLT ethics statement.
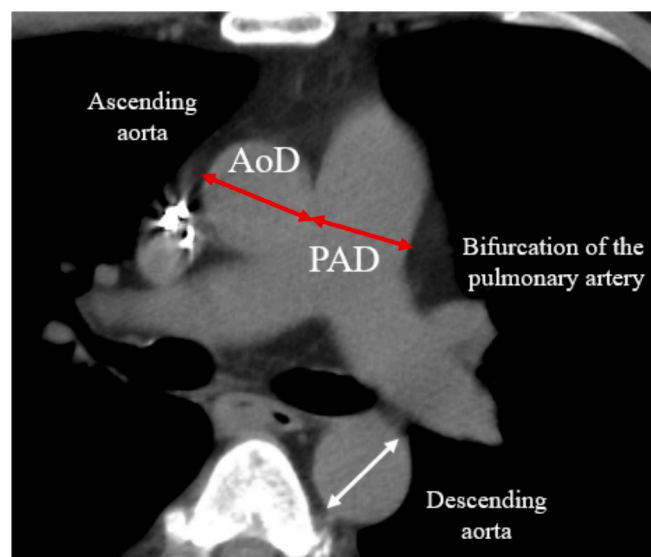

Fig. 1. Measurement of ascending aorta diameter and pulmonary artery diameter in computed tomography images.
The pulmonary artery diameter (PAD) and ascending aorta diameter (AoD) were assessed on a transverse computed tomography (CT) image at the level of the pulmonary artery bifurcation before LVAD implantation.

2.2. Protocol and analysis of CT images

Non-contrast CT studies were performed using a 320-detector row CT scanner (Aquilion ONE, Toshiba Medical Systems), a dual-source CT scanner (SOMATOM Definition Flash, SIEMENS) at Osaka University Hospital, and a 16-detector row CT scanner (ECLOS-16S, Hitachi Medico) at the Imperial Hotel Clinic, Osaka. CT images were obtained using a standard protocol [14] with a 5-mm slice thickness, 120 kVp, 70–450-mA tube current, and 400–800 msec exposure time. AoD and PAD were measured at the level of the main pulmonary artery bifurcation in transaxial slices (Fig. 1) [14,15]. For patients who underwent LVAD implantation, CT images were obtained within 90 days before the procedure, with a median of 17 days (25th and 75th percentiles, 6 and 38 days, respectively).

2.3. Echocardiography and right heart catheterization

Transthoracic echocardiographic indices were obtained using standard methods previously described by experienced sonographers [16]. For patients who underwent LVAD implantation, echocardiography was performed within 30 days before LVAD implantation, with a median time of 5 days (25th and 75th percentiles, 2 and 12 days, respectively). Tricuspid annular plane systolic excursion (TAPSE) was measured in the apical four-chamber view using M-mode to assess tricuspid lateral annulus motion. The RV end-diastolic diameter (RVDd) was defined as the maximal short-axis dimension in the basal one-third of the RV observed in the four-chamber view [17].

RHC was performed in 119 of the 141 patients (84 %) within 30 days before LVAD implantation, with a median time of 6 days (25th and 75th percentiles, 3 and 12 days, respectively). Pressure data, including pulmonary artery pressure (PAP), PAWP, and RAP, were obtained using a Swan–Ganz catheter, whereas cardiac output (CO) was determined using the Fick method. Additionally, pulmonary vascular resistance (PVR), RV stroke volume index (RVSWI), pulmonary artery pulsatility index (PAPi), diastolic pressure gradient (DPG), and transpulmonary gradient (TPG) were calculated as follows: PVR = (mean PAP - PAWP)/CO, RVSWI = (stroke volume index) x (mean PAP - RAP), PAPi = (systolic PAP – diastolic PAP)/RAP, DPG = diastolic PAP - PAWP, and TPG = mean PAP – PAWP [6,18–20].

Table 1
Baseline characteristics of the study population.

	Healthy individuals	Patients with LVAD implantation	p Value
	(*n* = 117)	(*n* = 141)	
General information			
Age, (years)	45.7 ± 8.5	46.9 ± 12.7	0.38
Male, n (%)	68 (58)	99 (70)	0.05
Height, (m)	1.66 ± 0.08	1.67 ± 0.09	0.96
Weight, (kg)	60.8 ± 11.8	58.6 ± 11.1	0.11
Body surface area (m²)	1.71 ± 0.19	1.69 ± 0.18	0.54
Systolic blood pressure (mmHg)	108.6 ± 14.5	94.3 ± 12.9	<0.01
Diastolic blood pressure (mmHg)	66.3 ± 9.7	58.2 ± 8.6	<0.01
Heart rate (beats/min)	63.4 ± 9.0	82.8 ± 14.8	<0.01
Echocardiography			
LVDd (mm)	46.0 ± 3.9	71.3 ± 12.0	<0.01
LVDs (mm)	30.3 ± 3.0	65.7 ± 13.0	<0.01
LVEF (%)	63.1 ± 3.8	19.6 ± 8.9	<0.01
Left atrial diameter, (mm)	29.7 ± 4.6	48.2 ± 10.3	<0.01
MR: none or trivial, n (%)	117 (100)	22 (15)	<0.01
TR: none or trivial, n (%)	117 (100)	39 (28)	<0.01

LVDd: left ventricular end-diastolic diameter; LVDs: left ventricular end-systolic diameter; LVEF: left ventricular ejection fraction; MR: mitral regurgitation; TR: tricuspid regurgitation.
Continuous data are expressed as the mean ± standard deviation for symmetrical variables and as the median (interquartile range) for nonsymmetrical variables, while categorical variables are expressed as crude numbers (%).

2.4. Statistical analyses

Data were analyzed using Student's *t*-test and one-way analysis of variance for normal continuous variables and the Wilcoxon–Mann–Whitney test for non-normal continuous variables. For categorical variables, the χ^2 test or Fisher's exact test was used. Tukey's test was used to compare the differences in PAD, AoD, and PAD/AoD ratios among healthy individuals, patients with RVF, and patients without RVF after LVAD implantation. Analysis of covariance was used to compare the intercepts and slopes of PAD and AoD among these groups. Decision tree analysis was performed to determine the variables and cutoff values that were most effective in predicting RVF after LVAD implantation. Optimal cutoff values were determined using the Youden Index at each classification step using Receiver Operating Characteristic analysis. The patients were automatically divided into two groups and then repeatedly assessed and divided according to the two-choice branching method. Branching was stopped when no additional significant variables were detected, and the number of patients was decreased to 10 to prevent overfitting. Statistical significance was determined using a two-tailed *p*-value of less than 0.05. The statistical software packages used for the analyses were JMP Pro 14.0.0 (SAS Institute, Cary, NC, USA) and GraphPad Prism Version 9.3.1 (GraphPad Prism Software Inc., San Diego, California).

3. Results

3.1. Baseline characteristics in patients who underwent LVAD implantation and in healthy individuals

Patients who underwent LVAD implantation had similar age, sex, and body surface area, which are major determinants of AoD [14], to those of the healthy subjects (Table 1). They had significantly lower blood pressure, a lower left ventricular ejection fraction (LVEF), a larger LV end-diastolic diameter (LVDd), and a larger left atrial diameter than healthy individuals.

Table 2
Preoperative clinical characteristics of the study population.

	RV failure	No-RV failure	p Value
	(*n* = 29)	(*n* = 112)	
General information			
Age, (years)	47.4 ± 11.5	46.8 ± 13.0	0.82
Male, n (%)	19 (66)	80 (71)	0.54
Height (m)	1.67 ± 0.09	1.67 ± 0.09	0.86
Weight (kg)	59.1 ± 12.5	58.4 ± 10.7	0.77
Body surface area (m²)	1.70 ± 0.19	1.69 ± 0.17	0.92
Body mass index (Kg/m²)	21.1 ± 4.0	20.8 ± 3.1	0.60
Follow-up duration (years)	5 (4–8)	5 (1–8)	0.41
Etiology of cardiomyopathy, n			
DCM / dHCM / ICM / others	10/12/2/5	77/13/13/9	<0.01
Hypertension, n (%)	2 (7)	10 (9)	0.72
Diabetes mellitus, n (%)	9 (31)	23 (20)	0.24
COPD, n (%)	0 (0)	2 (2)	0.34
Systolic blood pressure (mmHg)	93.7 ± 10.5	94.5 ± 13.5	0.79
Diastolic blood pressure (mmHg)	59.3 ± 6.5	57.9 ± 9.1	0.43
Heart rate (beats/min)	82.1 ± 15.2	82.9 ± 14.7	0.78
INTERMACS class, n (%)			0.30
1	1 (3)	1 (1)	
2	9 (31)	32 (29)	
3	19 (66)	76 (67)	
≥4	0 (0)	3 (3)	
Use of ≥3 inotropes, n (%)	3 (10)	12 (11)	0.95
Duration of inotropes, (days) (*n* = 123)	49 (27–102)	51 (27–93)	0.66
MCS, n (%)	13 (45)	30 (27)	0.07
Mechanical Ventilation, n (%)	5 (17)	12 (11)	0.35
Laboratory data			
Aspartate aminotransferase (IU/L)	24 (19–38)	25 (19–31)	0.53
Total bilirubin (mg/dL)	1.0 (0.7–1.9)	0.8 (0.6–1.2)	0.04
White blood cell count, 10*3/μl	7.6 ± 4.1	6.7 ± 2.8	0.18
Hemoglobin (g/dL)	12.0 ± 2.1	11.9 ± 1.9	0.71
Hematocrit (%)	36.1 ± 5.8	35.9 ± 5.5	0.82
Platelets 10*5/(μl)	1.8 ± 0.7	2.0 ± 0.7	0.34
Blood urea nitrogen (mg/dl)	17 (14–23)	17 (12–24)	0.83
Creatinine (mg/dL)	0.9 (0.8–1.1)	1.0 (0.8–1.3)	0.62
Serum Na (mEq/L)	135 (133–139)	136 (134–138)	0.92
Log BNP (pg/mL)	2.8 (2.5–2.9)	2.5 (2.2–2.8)	0.02
Total protein (g/dl)	6.8 (6.2–7.1)	7.0 (6.4–7.4)	0.06
Albumin (g/dl)	3.7 (3.1–4.1)	3.9 (3.4–4.2)	0.28
PT-INR s	1.4 ± 0.4	1.4 ± 0.4	0.48
Medications			
ACEI and/or ARB, n (%)	18 (62)	86 (77)	0.12
Beta-blockers, n (%)	27 (93)	102 (91)	0.72
Diuretics, n (%)	23 (79)	103 (92)	0.07
Mineralocorticoid receptor antagonists, n (%)	25 (86)	98 (88)	0.85
Echocardiography			
LVDd (mm)	66.2 ± 14.4	72.6 ± 11.0	<0.01
LVDd index (mm/m²)	40.1 ± 8.9	43.7 ± 6.4	0.01
LVEF, (%)	22.1 ± 10.6	18.9 ± 8.4	0.08
Left atrial diameter (mm)	50.0 ± 11.7	47.8 ± 9.9	0.29
TR pressure gradient (mmHg) (*n* = 130)	31.6 ± 14.0	31.1 ± 14.7	0.86
TAPSE (mm) (*n* = 99)	14.9 ± 4.3	15.3 ± 4.4	0.77
RVDd (mm) (*n* = 111)	41.3 ± 10.7	38.0 ± 11.0	0.20

RV: right ventricle; ACEI: angiotensin converting enzyme inhibitor; ARB: angiotensin II receptor blocker; BMI: body mass index; BNP: brain natriuretic peptide; COPD: chronic obstructive pulmonary disease; DCM: dilated cardiomyopathy; dHCM: dilated phase of hypertrophic cardiomyopathy; HF: heart failure; ICM: ischemic cardiomyopathy; MCS: mechanical circulatory support; INTERMACS: Interagency Registry for Mechanically Assisted Circulatory Support; PT-INR: prothrombin time international normalized ratio; RVDd: right ventricular end-diastolic diameter; TAPSE: tricuspid annular plane systolic excursion.
Continuous data are expressed as the mean ± standard deviation for symmetrical variables and as the median (interquartile range) for nonsymmetrical variables, while categorical variables are expressed as crude numbers (%).
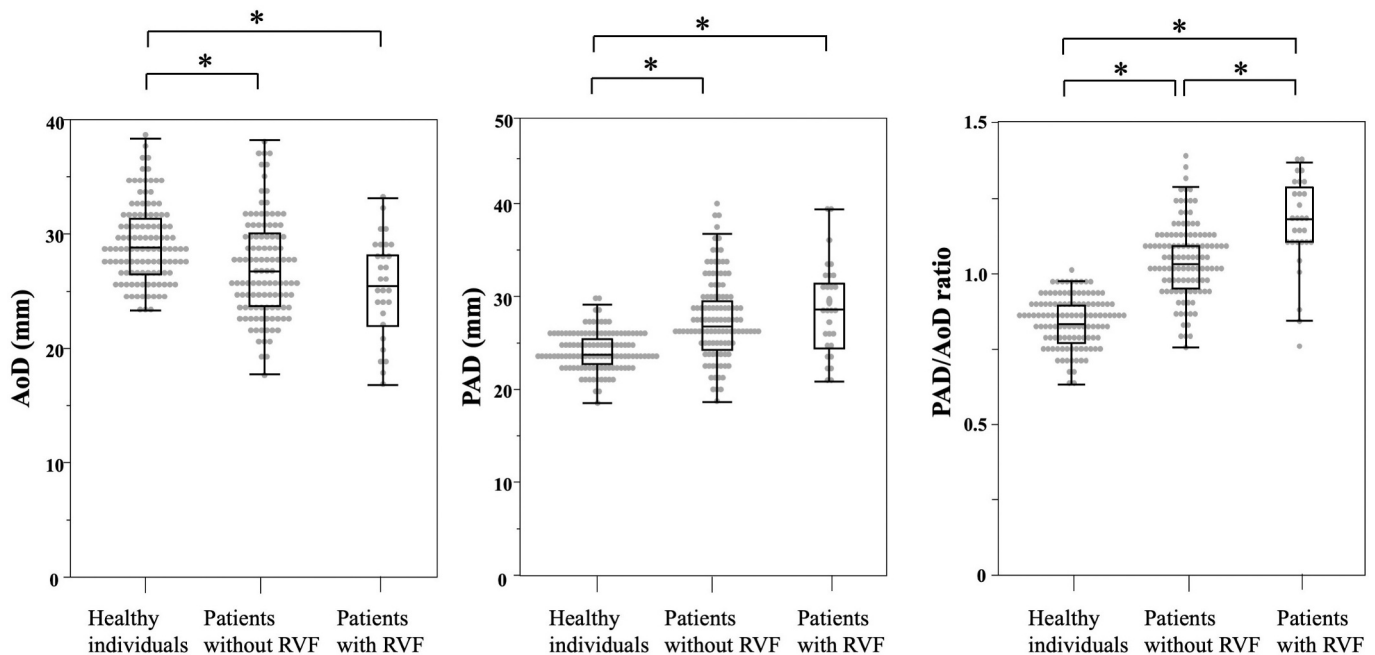
Fig. 2. AoD, PAD pulmonary artery diameter, and PAD/ AoD ratio in healthy individuals, the patients with and without RVF after LVAD implantation.
The ascending aorta diameter (AoD) (A), pulmonary artery diameter (PAD) (B), and PAD/AoD ratio (C) were significantly different between healthy individuals and patients with and without RVF after LVAD implantation (all $p < 0.01$). The PAD/AoD ratio was significantly different between the patients with and without RVF (p < 0.01); however, the AoD ($p = 0.11$) and PAD ($p = 0.24$) ratios were not. The horizontal line in the middle of each box indicates the median; the top and bottom borders of the box mark the 75th and 25th percentiles, and the whiskers mark the maximum and minimum points.
* p < 0.01; RVF: right ventricular failure; AoD: ascending aorta diameter; PAD: pulmonary artery diameter.

3.2. Baseline characteristics and RVF

Of the 141 patients who underwent LVAD implantation, 29 (21 %) experienced RVF, including eight cases of early acute RVF, and nine (6 %) required RVAD implantation. Table 2 shows a comparison of clinical characteristics, preoperative echocardiographic parameters, and laboratory data between patients with and without RVF. Patients with RVF were more likely to have smaller LVDd and LVDd index, higher total bilirubin levels, and higher log BNP levels than those without RVF (all $P < 0.05$). The LVEF, TAPSE, and RVDd were not significantly different between the two groups. Although patients with RVF had significantly higher RAP, lower PAPi, and higher RAP/PAWP ratios than those without RVF (all $p < 0.05$), the mean PAP, PVR, PAWP, CI, RVSWI, DPG, and TPG were not significantly different between the two groups (Supplemental Table S1).

AoD was significantly smaller, and PAD and PAD/AoD ratios were significantly larger in patients with and without RVF after LVAD implantation than in healthy individuals (Fig. 2). Although neither AoD nor PAD was significantly different between patients with and without RVF ($p = 0.11$, $p = 0.24$, respectively), the PAD/AoD ratio was significantly different between these groups ($p < 0.01$). Fig. 3 shows the distribution and correlation between AoD and PAD in each group. A comparison of the slopes of each line showed a statistically significant difference between patients with and without RVF, with higher slopes observed in comparison with healthy individuals ($p < 0.01$). However, there was no significant difference in the slopes between patients with and without RVF ($p = 0.63$). Additionally, the intercepts of the lines for patients with and without RVF were significantly different (p < 0.01).

3.3. Decision tree model of RVF after LVAD implantation

Table 3 presents the results of the univariate logistic analysis of the non-invasive parameters for predicting RVF after LVAD implantation. LVDd index, total bilirubin level, and PAD/AoD ratio were significantly

associated with RVF. The association between PAD/AoD ratio and RVF remained significant even after adjusting for LVDd index, and total bilirubin level ($p < 0.01$). The PAD/AoD ratio was also associated with early acute RVF alone (odds ratio: 1.06, 95 % confidence interval: 1.00–1.11, $p = 0.04$). Fig. 4 shows the results of the decision tree analysis. The first predictor was the PAD/AoD ratio, with a cutoff value of 1.09. The incidence of RVF after LVAD implantation was 6 % in patients with a low PAD/AoD ratio (<1.09) and 47 % in patients with a high PAD/AoD ratio (≥ 1.09). For patients with a low PAD/AoD ratio (<1.09), the second predictor was log BNP, with a cutoff value of 2.79 (617 pg/ml). The incidence of RVF was 22 % in patients with a high log BNP (≥ 2.79) and 1 % in patients with a low log BNP (<2.79). For patients with a high PAD/AoD ratio (≥ 1.09), the second predictor was the LVDd index, with a cutoff value of 35.4 mm/m². The incidence of RVF was 34 % in patients with a large LVDd index (≥ 35.4 mm/m²) and 100 % in patients with a small LVDd index (<35.4 mm/m²). The probability of RVF varied greatly among the four subgroups based on the decision tree analysis. The subgroup with a high PAD/AoD ratio (≥ 1.09) and a small LVDd index (<35.4 mm/m²) had the highest probability of RVF (100 %), while the subgroup with a low PAD/AoD ratio (<1.09) and a low log BNP (<2.79) showed the lowest probability of RVF (1 %).

4. Discussion

This study has three major findings. First, patients with and without RVF after LVAD implantation had significantly smaller AoD, enlarged PAD, and higher PAD/AoD ratios than healthy individuals. Second, although neither AoD nor PAD was significantly different between patients with and without RVF, the PAD/AoD ratio was significantly different. Third, the PAD/AoD ratio, LVDd, LVDd index, total bilirubin level, and log BNP level were associated with RVF after LVAD implantation. Using decision tree analysis with these variables, we found that a high PAD/AoD ratio (≥ 1.09), a small LVDd index (<35.4 mm/m²), and a high log BNP value (≥ 2.79) were predictors of RVF after LVAD
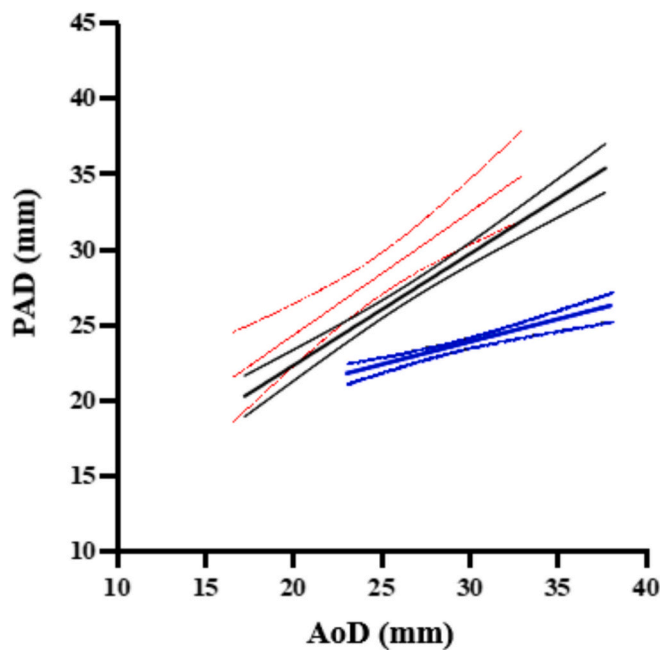
Fig. 3. The correlations between AoD and PAD in healthy individuals, the patients with and without RVF after LVAD implantation.
The regression line between the ascending aorta diameter (AoD) and the pulmonary artery diameter (PAD) in patients with right ventricular failure (RVF) is indicated by red lines, that in patients without RVF by black lines, and that in healthy individuals by blue lines. The slopes of the lines in patients with RVF were higher than those in healthy individuals (p < 0.01). Similarly, the slopes of patients without RVF were higher than those of healthy individuals (p < 0.01). However, there was no significant difference in the slopes between the patients with and without RVF ($p = 0.63$). In contrast, the intercepts of the lines in patients with and without RVF were significantly different (p < 0.01). Each outline represents the estimated 95 % confidence upper and lower limits.

Table 3
Univariate logistic Analyses for Predictors of RVF.

	OR (95 % CI)	p Value
Age, per one-year increase	1.00 (0.97–1.04)	0.82
Male	1.32 (0.54–3.14)	0.54
Total bilirubin per 1 g/dl increase	1.80 (1.06–3.06)	0.03
Log BNP per 0.1unit increase	1.10 (0.99–1.22)	0.06
LVDd index per 1 mm unit decrease	0.93 (0.87–0.99)	0.01
PAD/AoD ratio per 0.01 increase	1.08 (1.04–1.12)	<0.01

AoD: ascending aorta diameter; BNP: brain natriuretic peptide; CI: confidence interval; LVDd: left ventricular end-dilated diameter; OR: odds ratio; PAD: pulmonary artery diameter.

implantation. These factors allowed us to categorize the patients into four subgroups with varying rates of RVF, ranging from 1 % to 100 %. The subgroup with a high PAD/AoD ratio (≥1.09) and small LVDd index (<35.4 mm/m^2) had the highest probability of RVF (100 %), while the subgroup with a low PAD/AoD ratio (<1.09) and low log BNP value (<2.79) had the lowest probability of RVF (1 %). These findings suggest that non-invasive parameters can be used to evaluate the risk of RVF after LVAD implantation.

Recent studies have attempted to determine which clinical indices are effective preoperative predictors because RVF after LVAD implantation deteriorates a patient's quality of life and prognosis. Assessment of RV function using RHC parameters has become the standard method because it provides information about RV function that is not always predictable from morphological assessments. RAP, RAP/PAWP, CI, RVSWI, PVR, and PAPi have been reported to be useful in predicting RVF after LVAD implantation [10,18–23]. In this study, a high RAP/

PAWP ratio, low PAPi, and high RAP were associated with RVF. In this study, log BNP was moderately correlated with RAP ($r = 0.45$, $p < 0.01$) and weakly correlated with PAPi and RAP/PAWP ratio ($r = -0.23$, p < 0.01, $r = 0.22$, p < 0.01, respectively). Within the patients with a low PAD/AoD ratio, those with a low log BNP had a significantly lower RAP value than those with a high log BNP (5.2 ± 3.7 mmHg vs. 8.9 ± 4.7 mmHg, p < 0.01). High BNP levels were associated with RVF after LVAD implantation in previous studies [22,24]. Which is consistent with this study. In the non-invasive RVF prediction model used in this study, BNP may play an alternative role to invasive hemodynamic parameters. However, hemodynamic data may also be informative when combined with noninvasive evaluations. Although the number of patients was limited, it was possible to use hemodynamic parameters to reclassify the probability of RVF in patients with intermediate probabilities according to the decision tree evaluation using noninvasive parameters (Supplemental Fig. S1).

The preoperative RV sphericity index, TAPSE using tissue Doppler imaging, and RV longitudinal strain using the speckle-tracking method have been reported as useful predictors of RVF after LVAD implantation [25,26]. However, echocardiographic evaluation is not reproducible and susceptible to differences among examiners, especially those related to RV assessment [27]. RVF after LVAD implantation is influenced by changes in the shape of the right ventricle as well as decreased contractile and diastolic function due to the shift of the interventricular septum towards the left ventricle as a result of the unloading of the left ventricle by the LVAD. Several studies have indicated that this phenomenon is particularly likely to occur when LVDd is relatively small [22,28,29]. Imamura et al. previously reported that LVDd less than 64 mm was a significant risk factor for RVAD implantation [29]. In this study, the LVDd and LVDd index were significantly associated with RVF after LVAD implantation. The LVDd and LVDd index may be good indicators of RV function because volumetric loading of the LV is influenced by the stroke volume of the RV.

We have previously found a significant relationship between smaller AoDs and lower CO in patients with advanced HF [11]. Other reports have shown that an enlarged PAD, as assessed using non-contrast CT scans, is associated with increased PA pressure and has excellent diagnostic value for detecting PH [30,31]. AoD and PAD do not vary by temporal hemodynamic changes [11]. Patients with severe HF who require LVAD implantation often have reduced CO for an extended period and develop postcapillary PH. Such prolonged postcapillary PH commonly causes severe damage to the RV myocardium and an enlarged PAD [6–8,30,31]. Severe damage to the RV myocardium leads to a decrease in the CO, resulting in a smaller AoD. In other words, a small AoD may indicate prolonged low CO associated with severe dysfunction of the right and/or left ventricles, and an enlarged PAD may indicate prolonged postcapillary PH (Supplemental Fig. S2). However, PAD may be reduced by very low SV of the RV in patients with severely impaired RV function. A noticeable variation in PAD was evident in patients from this study with low SV and presenting RVF after LVAD. This, in turn, suggests differences in the onset or the total duration of RV dysfunction. Although serial PAD, AoD, and RV function data are needed to evaluate this hypothesis, the PAD/AoD ratio may be a comprehensive index capable of reflecting the history of impaired hemodynamics and cardiac function.

4.1. Limitations

This study had several limitations. First, it was a single-center retrospective study, which may have diminished the power of our statistical inferences. Second, we did not evaluate 24 % of the patients with primary LVAD implantation because of the lack of CT data, which might have led to bias in the patient population. However, the key patient characteristics and the incidence of RVF were similar (Supplemental Table S2). Third, we did not investigate the associations between the etiologies of RVF and PAD, AoD, or the PAD/AoD ratio due to the lack of
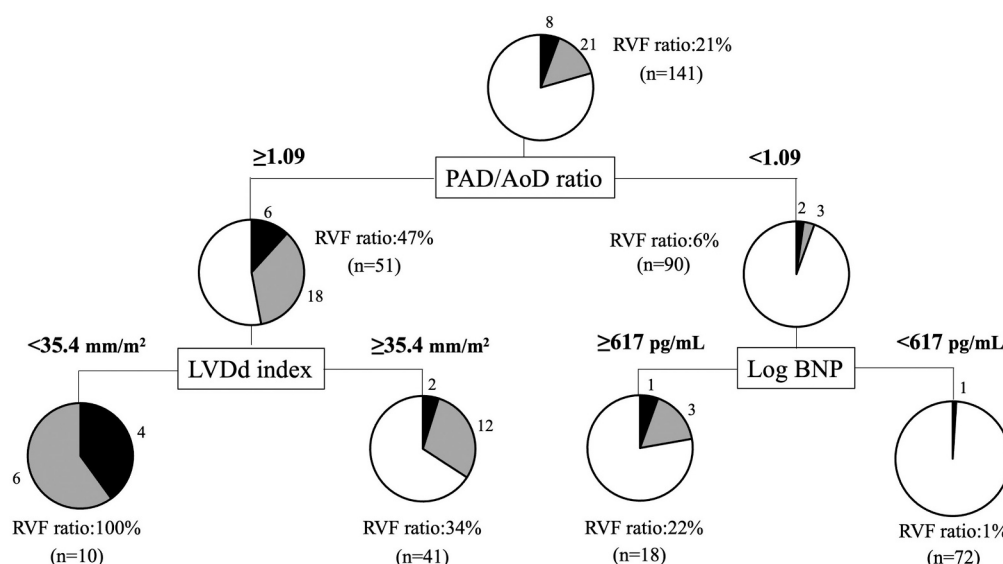
Fig. 4. Decision tree model of RVF after LVAD implantation.
Noninvasive variables which showed significant differences in Table 2 were evaluated as splitting factors. Given that LVDd and LVDd index were highly correlated, LVDd index was adopted considering sex difference. Boxes indicate the splitting factors. Pie charts indicate RVF rates after LVAD implantation in each group (Subtypes of RVF; Black: early acute RVF; Gray: early post-LVAD RVF).
BNP: brain natriuretic peptide; LVDd: left ventricular end-diastolic diameter.

established variables capable of determining the etiology of RVF. However, our results suggest that ventricular interdependence and the involvement of RV cardiomyopathy contribute to the development of RVF. Finally, the LVAD type may have affected the incidence of RV dysfunction after LVAD implantation.

5. Conclusion

The PAD/AoD ratio is a simple and non-invasive indicator of the risk of RVF after LVAD implantation. By combining non-invasive hemodynamic parameters, such as log BNP, with non-invasive non-hemodynamic parameters, such as the PAD/AoD ratio or LVDd index, the likelihood of RVF after LVAD implantation can be predicted with high accuracy.

Declaraion of competing interest

The authors declare that they have no conflicts of interest.

Funding

CRediT authorship contribution statement

Misato Chimura: Writing – original draft, Visualization, Formal analysis, Data curation, Conceptualization. **Tomohito Ohtani:** Writing – review & editing, Visualization, Supervision, Project administration, Formal analysis. **Fusako Sera:** Supervision, Investigation. **Kei Nakamoto:** Investigation. **Yasuhiro Akazawa:** Investigation. **Kenji Kajitani:** Investigation, Supervision. **Rie Higuchi:** Investigation, Supervision. **Toshifumi Kagiya:** Writing – review & editing, Investigation, Supervision. **Yasushi Sakata:** Writing – review & editing, Supervision, Funding acquisition.

Acknowledgements

Appendix A. Supplementary data

Supplementary data to this article can be found online at https://doi.org/10.1016/j.ijcard.2024.132596.

References

[1] O.H. Frazier, E.A. Rose, M.C. Oz, et al., Multicenter clinical evaluation of the HeartMate vented electric left ventricular assist system in patients awaiting heart transplantation, J. Thorac. Cardiovasc. Surg. 122 (2001) 1186–1195.

[2] O. Wever-Pinzon, S.G. Drakos, A.G. Kfoury, et al., Morbidity and mortality in heart transplant candidates supported with mechanical circulatory support: is reappraisal of the current united network for organ sharing thoracic organ allocation policy justified? Circulation 127 (2013) 452–462.

[3] F.D. Pagani, L.W. Miller, S.D. Russell, et al., Extended mechanical circulatory support with a continuous-flow rotary left ventricular assist device, J. Am. Coll. Cardiol. 54 (2009) 312–321.

[4] T. Nakatani, K. Sase, H. Oshiyama, et al., Japanese registry for mechanically assisted circulatory support: first report, J. Heart Lung Transplant. 36 (2017) 1087–1096.

[5] C. Lo, D. Murphy, R. Summerhayes, et al., Right ventricular failure after implantation of continuous flow left ventricular assist device: analysis of predictors and outcomes, Clin. Transpl. 29 (2015) 763–770.

[6] V.P. Harjola, A. Mebazaa, J. Čelutkienė, et al., Contemporary management of acute right ventricular failure: a statement from the heart failure association and the working group on pulmonary circulation and right ventricular function of the European Society of Cardiology, Eur. J. Heart Fail. 18 (2016) 226–241.

[7] B.A. Houston, K.B. Shah, M.R. Mehra, R.J. Tedford, A new "twist" on right heart failure with left ventricular assist systems, J. Heart Lung Transplant. 36 (2017) 701–707.

[8] F. Haddad, S.A. Hunt, D.N. Rosenthal, D.J. Murphy, Right ventricular function in cardiovascular disease, part I: anatomy, physiology, aging, and functional assessment of the right ventricle, Circulation 117 (2008) 1436–1448.

[9] O.I.I. Soliman, S. Akin, R. Muslem, et al., EUROMACS investigators. Derivation and validation of a novel right-sided heart failure model after implantation of continuous flow left ventricular assist devices: the EUROMACS (European registry for patients with mechanical circulatory support) right-sided heart failure risk score, Circulation 137 (2018) 891–906.

[10] R.L. Kormos, J.J. Teuteberg, F.D. Pagani, et al., HeartMate II clinical investigators. Right ventricular failure in patients with the HeartMate II continuous-flow left ventricular assist device: incidence, risk factors, and effect on outcomes, J. Thorac. Cardiovasc. Surg. 139 (2010) 1316–1324.

[11] M. Chimura, T. Ohtani, Y. Tsukamoto, et al., Ratio of pulmonary artery diameter to ascending aortic diameter and severity of heart failure, J. Heart Lung Transplant. 37 (2018) 1341–1350.

[12] N. Kashiyama, K. Toda, T. Nakamura, et al., Evaluation of right ventricular function using liver stiffness in patients with left ventricular assist device, Eur. J. Cardiothorac. Surg. 51 (2017) 715–721.

[13] R.L. Kormos, C.F.J. Antonides, D.J. Goldstein, et al., Updated definitions of adverse events for trials and registries of mechanical circulatory support: a consensus statement of the mechanical circulatory support academic research consortium, J. Heart Lung Transplant. 39 (2020) 735–750.

[14] A. Wolak, H. Gransar, L.E. Thomson, et al., Aortic size assessment by noncontrast cardiac computed tomography: normal limits by age, gender, and body surface area, JACC Cardiovasc. Imaging 1 (2008) 200–209.

[15] J.M. Wells, G.R. Washko, M.K. Han, et al., Pulmonary arterial enlargement and acute exacerbations of COPD, N. Engl. J. Med. 367 (2012) 913–921.

[16] R.M. Lang, L.P. Badano, V. Mor-Avi, et al., Recommendations for cardiac chamber quantification by echocardiography in adults: an update from the American Society of Echocardiography and the European Association of Cardiovascular Imaging, J. Am. Soc. Echocardiogr. 28 (2015) 1–39.e14.

[17] L.G. Rudski, W.W. Lai, J. Afilalo, et al., Guidelines for the echocardiographic assessment of the right heart in adults: a report from the American Society of Echocardiography endorsed by the European Association of Echocardiography, a registered branch of the European Society of Cardiology, and the Canadian Society of Echocardiography, J. Am. Soc. Echocardiogr. 23 (2010) 685–713.

[18] T. Ibe, H. Wada, K. Sakakura, et al., Right ventricular stroke work index, Int. Heart J. 59 (2018) 1047–1051.

[19] G. Kang, R. Ha, D. Banerjee, Pulmonary artery pulsatility index predicts right ventricular failure after left ventricular assist device implantation, J. Heart Lung Transplant. 35 (2016) 67–73.

[20] H. Alnsasra, R. Asleh, S.D. Schettle, et al., Diastolic pulmonary gradient as a predictor of right ventricular failure after left ventricular assist device implantation, J. Am. Heart Assoc. 8 (2019) e012073.

[21] Y. Ochiai, P.M. McCarthy, N.G. Smedira, et al., Predictors of severe right ventricular failure after implantable left ventricular assist device insertion: analysis of 245 patients, Circulation 106 (2002) I198–I202.

[22] T. Shiga, K. Kinugawa, T. Imamura, et al., Combination evaluation of preoperative risk indices predicts requirement of biventricular assist device, Circ. J. 76 (2012) 2785–2791.

[23] M. Dandel, E. Potapov, T. Krabatsch, et al., Load dependency of right ventricular performance is a major factor to be considered in decision making before ventricular assist device implantation, Circulation 128 (2013) S14–S23.

[24] T.S. Kato, A. Chokshi, P. Singh, et al., Markers of extracellular matrix turnover and the development of right ventricular failure after ventricular assist device implantation in patients with advanced heart failure, J. Heart Lung Transplant. 31 (2012) 37–45.

[25] M. Cameli, M. Lisi, F.M. Righini, et al., Speckle tracking echocardiography as a new technique to evaluate right ventricular function in patients with left ventricular assist device therapy, J. Heart Lung Transplant. 32 (2013) 424–430.

[26] T.S. Kato, J. Jiang, P.C. Schulze, et al., Serial echocardiography using tissue Doppler and speckle tracking imaging to monitor right ventricular failure before and after left ventricular assist device surgery, JACC Heart Fail. 1 (2013) 216–222.

[27] M.D. Puchalski, R.V. Williams, B. Askovich, L.L. Minich, C. Mart, L.Y. Tani, Assessment of right ventricular size and function: echo versus magnetic resonance imaging, Congenit. Heart Dis. 2 (2007) 27–31.

[28] J.H. Karimov, G. Sunagawa, D. Horvath, K. Fukamachi, R.C. Starling, N. Moazami, Limitations to chronic right ventricular assist device support, Ann. Thorac. Surg. 102 (2016) 651–658.

[29] T. Imamura, K. Kinugawa, N. Kato, et al., Late-onset right ventricular failure in patients with preoperative small left ventricle after implantation of continuous flow left ventricular assist device, Circ. J. 78 (2014) 625–633.

[30] A.L. Chan, M.M. Juarez, D.K. Shelton, et al., Novel computed tomographic chest metrics to detect pulmonary hypertension, BMC Med. Imaging 11 (2011) 7.

[31] N. Corson, S.G. Armato 3rd, Z.E. Labby, C. Straus, A. Starkey, M. Gomberg-Maitland, CT-based pulmonary artery measurements for the assessment of pulmonary hypertension, Acad. Radiol. 21 (2014) 523–530.